

BIOMECHANICAL BEHAVIOR OF THE HYBRID ALL-ON-4 TECHNIQUE WITH SMOOTH ZYGOMATIC IMPLANTS AND EXTRA-LONG IMPLANTS WITH TRANSNASAL ANCHORAGE: A FINITE ELEMENT ANALYSIS



<https://doi.org/10.56238/arev6n4-491>

Submitted on: 11/31/2024

Publication date: 12/31/2024

Marcio Elias Francês Brito¹, Felipe Carvalho de Macêdo², Wesly Mejia Manrique³, Caio Marcio Eberhart Filho⁴, Ertton Massamitsu Miyasawa⁵, Luis Eduardo Marques Padovan⁶ and Leandro Eduardo Klüppel⁷.

ABSTRACT

The rehabilitation of patients with severely atrophic maxilla is a challenge and the hybrid all-on-4 technique emerges as an alternative for the treatment of these patients. This study aimed to evaluate the mechanical behavior of the rehabilitation of a severely atrophic total edentulous maxilla using smooth zygomatic implants and extra-long transnasal implants. Finite element analysis was conducted in the following configuration: two 3.75x45 mm Zygoma-S® implants installed using the sinus duct technique. 60 and 52 degree Mini Conical Abutment components with 1.5 mm gingival height were positioned in the regions of teeth 16 and 26 respectively. Two Helix Long GM® 3.75x20 mm and Components Mini Straight Conical Pillar with gingival height 1.5 mm were installed in the anterior region using the transnasal technique. A prosthetic bar was shaped and retained by 4 screws with a 12 mm cantilever. The peak stresses on the bone, implant, prosthetic component, and screws were below the strength limits of the materials. In addition, higher stresses were found in the zygomatic implants. Conversely, higher tensions were found in the thread region of the prosthetic components associated with the extra-long implants. The present study revealed that the rehabilitation of severely atrophic maxillae by the hybrid all-on-4 technique using two zygomatic implants and two extra-long implants with transnasal anchorage is biomechanically favorable and reliable.

Keywords: Dental Implant. Maxilla Edentula. Finite Element Analysis.

¹ Master in Implant Dentistry – ILAPEO College
LATTES: <http://lattes.cnpq.br/9157625426545050>

² Master in Implant Dentistry – ILAPEO College
LATTES: <http://lattes.cnpq.br/2431984612708427>

³ Mestranda in Implantodontics – Faculdade ILAPEO
LATTES: <https://lattes.cnpq.br/0361464337499735>

⁴ Undergraduate student in Medicine - Pontifical Catholic University of Paraná
LATTES: <http://lattes.cnpq.br/1957663430381093>

⁵ Professor - ILAPEO College
LATTES: <http://lattes.cnpq.br/0725700539300078>

⁶ Professor – ILAPEO College
LATTES: <http://lattes.cnpq.br/8506423321202833>

⁷ Professor Doctor - ILAPEO College
LATTES: <http://lattes.cnpq.br/9559429377225870>

INTRODUCTION

The rehabilitation of severely atrophic maxillae is a challenge due to the alterations that occur in these cases, such as pneumatization of the maxillary sinuses and the amount of bone in the maxilla that is insufficient for anchorage of conventional implants(1). Bone grafting procedures to try to restore bone volume to this patient have several disadvantages, such as risk of morbidity in the donor area, high costs and long duration of treatment(2).

As an alternative, different techniques have been developed involving anchoring implants in anatomical structures adjacent to the maxilla(3). Zygomatic implants have been used for years as an alternative to conventional implants in cases of atrophic maxilla. There are different techniques for implant placement. However, in the absence of bone availability for the installation of conventional implants by this technique, the installation of two extra-long implants with transnasal anchorage is an option(4).

Finite element analysis (FEA) is a computational method to predict the mechanical behavior of models through mathematical functions applied to geometries containing element meshes(5). This simulation is used in several areas of knowledge and has been applied in implant dentistry for decades. It is a reliable method that can provide understanding for clinical issues. There are few studies in the literature that evaluate the mechanical behavior of zygomatic implants associated with transnasal implants in severely atrophic maxilla. Thus, this study aimed to evaluate the mechanical behavior of the rehabilitation of a severely atrophic total edentulous maxilla using smooth zygomatic implants and transnasal extra-long implants.

MATERIALS AND METHODS

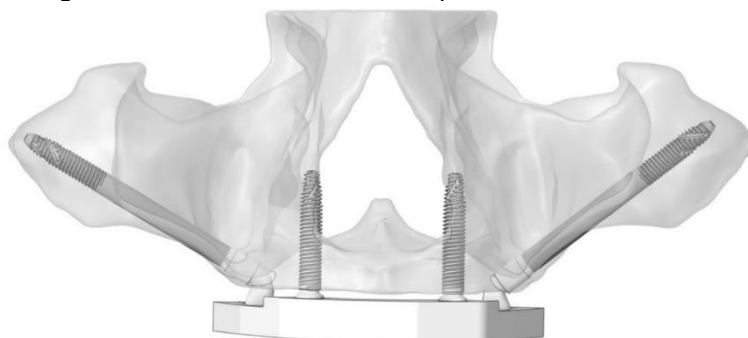
MODELING

Three-dimensional (3D) models of the maxilla, zygomatic bone, implants, prosthetic components and superstructure were used to evaluate the amount and distribution of stresses on the implants and underlying bone tissue. The 3D models of the maxilla and zygomatic bone were developed by simulating a fully edentulous patient with severe bone resorption. This model was created using Invesalio (Centro de Tecnologia da Informação Renato Archer, Brazil), Autodesk® MeshMixer™ (Autodesk, Inc), Ansys SpaceClaim (Ansys, Inc), and Autodesk Inventor (Autodesk, Inc) software. The geometries of the

implants, prosthetic components and screws were supplied by the manufacturer Neodent® (Curitiba, Paraná, Brazil).

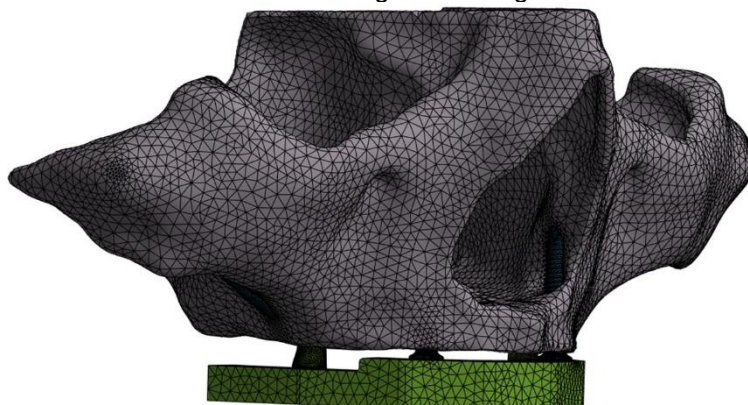
The FEA was performed in the following configuration: two 3.75x45 mm Zygoma-S® implants (Neodent®, Curitiba, Brazil) installed using the duct technique(6). Components of 60 and 52 degree Mini Conical Abutments with gingival height of 1.5 mm (Neodent®, Curitiba, Brazil) were positioned in the regions of teeth 16 and 26, respectively. Two Helix Long GM® 3.75x20 mm (Neodent®, Curitiba, Brazil) and Mini Tapered Straight Abutment Components with gingival height 1.5 mm were installed in the anterior region using the transnasal technique. A prosthetic bar was modeled with dimensions of 5 mm in the region of the lowest height by 7 mm wide and retained by 4 screws with a 12 mm cantilever (Figure 1).

Figure 1 – Three-dimensional model of the fully edentulous maxilla with 2 Zygoma-S implants®, two Helix Long GM® implants and angled Mini Conical Abutment components.



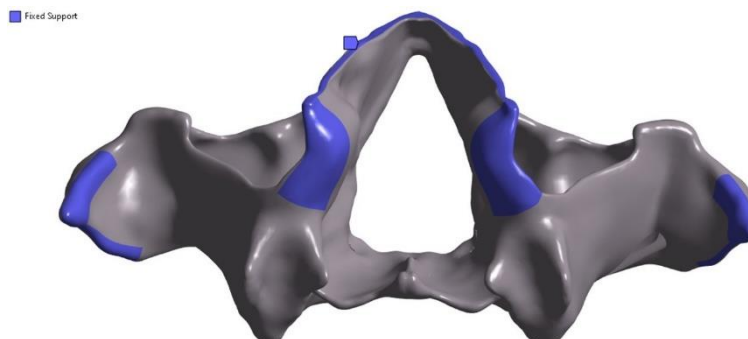
Mathematical models were created by dividing complex geometric models into simple and small elements. Hexahedral elements were used in the region of the screw body and tetrahedral elements were used in the other areas of the model. In total, 1,734,873 nodes and 1,121,174 elements were created (Figure 2).

Figure 2 – Mathematical model showing the mesh generated for the simulation.



The implant-bone interface was found to be perfectly bonded to simulate complete osseointegration. For the other interfaces, friction-type contacts were considered. The regions shown in Figure 3 were also fixed by simulating the connection with the skull and stabilizing the model during the application of force. This choice constrains the movement in all three directions (x, y, z) and their corresponding rotations.

Figure 3 – Representation of the fixation and restriction areas that stabilize the model during the application of forces.



FINITE ELEMENT ANALYSIS

Through the finite element methodology, it is possible to analyze the distribution of stresses in bone tissue, implants, components and screws. This distribution is evaluated by von Mises tensions.

The models previously built using CAD software were processed and exported to the software for finite element analysis (ANSYS 2023, Workbench, Canonsburg, PA, USA). After importation of the models, the loading condition as isometric bilateral bite and the magnitude of the force applied was 100N, in the cantilever region.

In the finite element analysis, three types of materials were considered: type II bone, grade IV titanium for the implants, and Ti6Al4V-ELI alloy titanium for the metal bar, Mini

Conical Abutment components, and screws (Table 1). The mechanical properties of each component used were defined based on the scientific literature and standards (Table 1). The mechanical properties required were modulus of elasticity and Poisson coefficient of each material, assuming an isotropic, homogeneous and linear elastic mechanical behavior.

Table 1 – Properties of the materials included in the finite element analysis

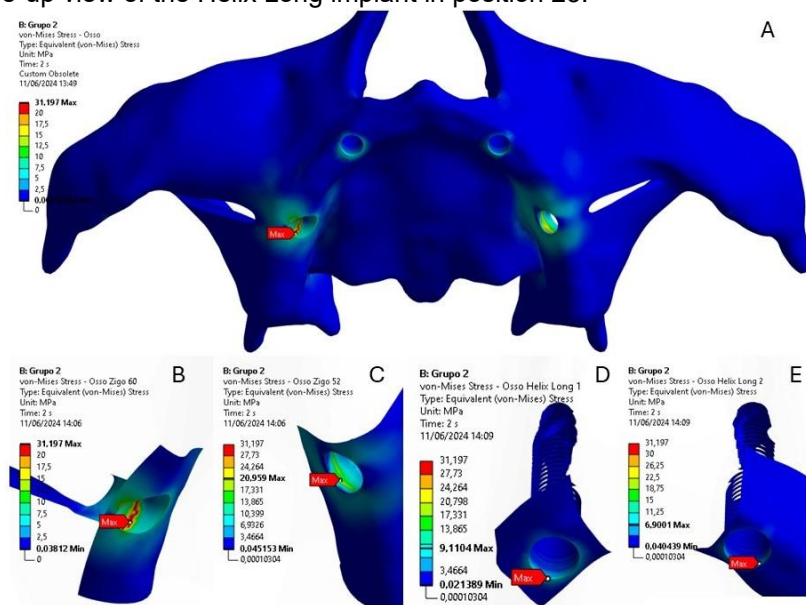
Properties of materials				
Material	Modulus of Elasticity – (MPa) - Stiffness	Tensile Limit (MPa)	Poisson coefficient (ν)	References
Bone type II	5500	170 (compression)	0,3	Tada et al. (2003) (7) Almeida et al. (2010) (8)
Titanium grade IV	110000	483 (minimum)*	0,35	ASTM F 67 Menacho-Mendoza et al. (2022) (9)
Ti6Al4V-ELI (titânio liga)	110000	795 (minimum)*	0,35	ASTM F 163 Zhang & Wang (2023) (10) Wang, Fu & Deng (2015) (11)
Interface				
Materials	Nature of the interface		Coefficient of friction	References
Bone x implant	Brew		-	Eskitascioglu et al. (2004) (12)
Implant x prosthetic component x prosthetic parafuse x prosthetic bar	Friction		0,2	Haack et al. (1995) (13) Lang et al. (2003) (14)

*Minimum values defined in the standard. In practice, the raw materials used by manufacturers can reach much higher values.

RESULTS

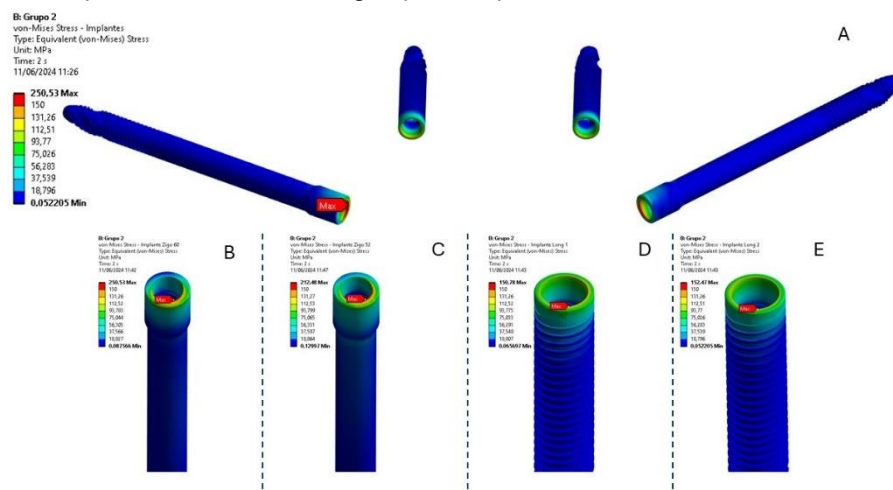
The stress distribution in the bone tissue reached a peak of 31.197 MPa located in the interface region with the collar of the Zygomatic Implant associated with the 60° Mini Conical Abutment in position 16 (Figures 4A and B). The maximum tension in the bone tissue adjacent to the zygomatic implant associated with the 52° Mini Conical Abutment in position 26 was 20,959 MPa (Figure 4C). It is possible to observe that the maximum tension in the bone tissue adjacent to the transnasal implants (9,110 MPa and 6,900 MPa) was at least 3 times lower than in the one adjacent to the zygomatic implants, also located in the region of interface with the implant collar (Figures 4D and E).

Figure 4 – Distribution of stresses on the cortical bone during loading. The red areas mean higher values and the blue ones, smaller. A) Palatine vision of the maxilla; B) Approximate view of the Zygoma-S implant associated with the 60° Mini Conical Abutment in position 16; C) Approximate view of the Zygoma-S implant associated with the 52° Mini Conical Abutment in position 26; D) Close view of the Helix Long implant in position 13; E) Close-up view of the Helix Long implant in position 23.



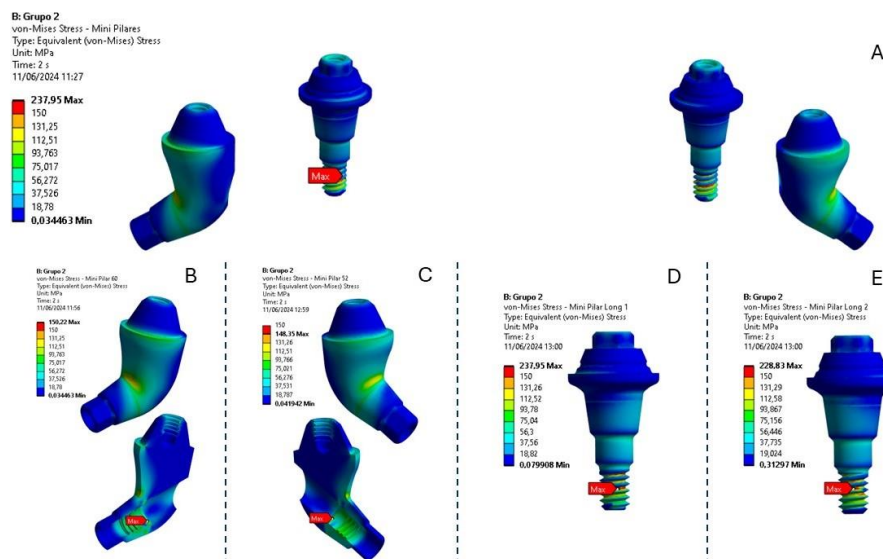
By analyzing the stress distribution in the system's implants, it is possible to identify a maximum peak voltage of 250.53 MPa located in the palatal region of the Zygomatic Implant cone associated with the 60° Mini Conical Abutment in position 16 (Figures 5A and B). The zygomatic implant associated with the 52° Mini Conical Abutment in position 26 had a lower maximum tension (212.48 MPa) than the other zygomatic implant and with maximum tension in the same palatal region of the implant cone (Figure 5C). The maximum tensions in the transnasal implants were similar, 150.78 MPa and 152.47 MPa in the implants in regions 13 and 23, respectively (Figures 5D and E).

Figure 5 - Stress distribution in the implants. The red areas mean higher values and the blue ones, smaller. A) Overview with all implants in the installation position; B) Approximate view of the Zygoma-S implant associated with the 60° Mini Conical Abutment in position 16; C) Approximate view of the Zygoma-S implant associated with the 52° Mini Conical Abutment in position 26; D) Close view of the Helix Long implant in position 13; E) Close-up view of the Helix Long implant in position 23.



The maximum tension found in the prosthetic components was 237.95 MPa in the thread region of the straight Mini Conical Abutment associated with the transnasal implant in region 13 (Figures 6A and D). A similar tension of 228.83 MPa was also found in the thread of the straight Mini Conical Abutment associated with the transnasal implant in region 23 (Figure 6E). Regarding the prosthetic components associated with zygomatic implants, the maximum stresses were 150.22 MPa and 148.34 MPa located in the elbow region of the component and in the region of the screw seating in the 60° and 52° Mini Conical Abutments, respectively (Figures 6B and C).

Figure 6 - Stress distribution in the prosthetic components. The red areas mean higher values and the blue ones, smaller. A) Overview of all prosthetic components in the installation position; B) Approximate view of the 60° Mini Conical Abutment associated with the Zygoma-S implant in position 16; C) Approximate view of the 52° Mini Conical Abutment associated with the Zygoma-S implant in position 26; D) Approximate view of the Mini Tapered Pillar E) Approximate view of the straight Mini Conical Abutment associated with the Helix Long implant in position 23.



The stress distribution in the screws of the angled Mini Conical Pillars was similar, being slightly higher in the screw of the 60° component with a maximum tension of 129.77 MPa (Figure 7). In relation to the prosthetic screws, maximum stresses were all in the same region of the interface between the screw head and the body, ranging from 134.26 to 202.28 MPa (Figure 8).

Figure 7 - Stress distribution in the screws of the angled prosthetic components. The red areas mean higher values and the blue ones, smaller. A) Overview of all the screws of the angled prosthetic components in the installation position; B) Close-up view of the screw of the Mini Tapered Abutment C) Close-up view of the screw of the straight Mini Conical Abutment associated with the Helix Long implant in position 23.

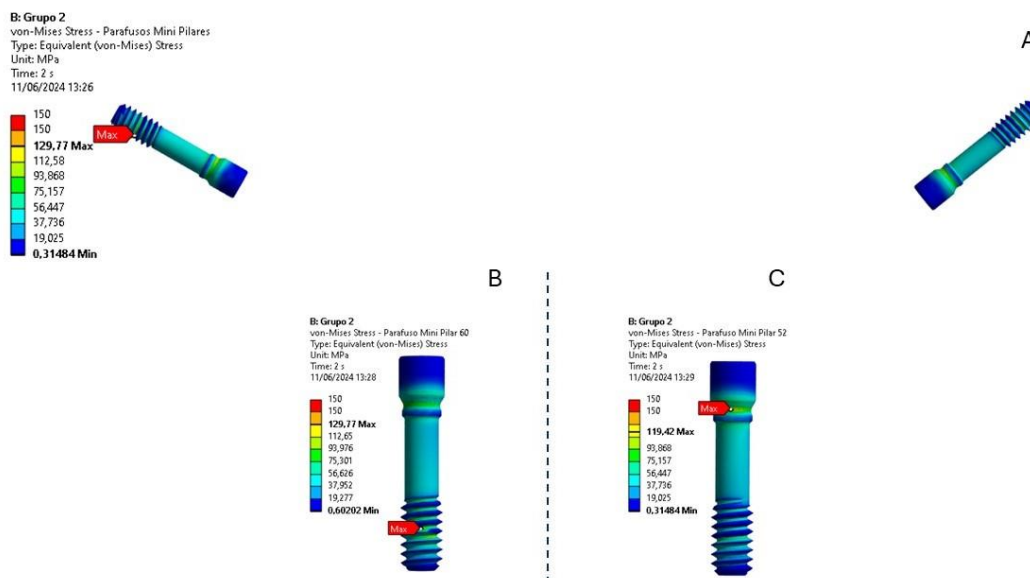
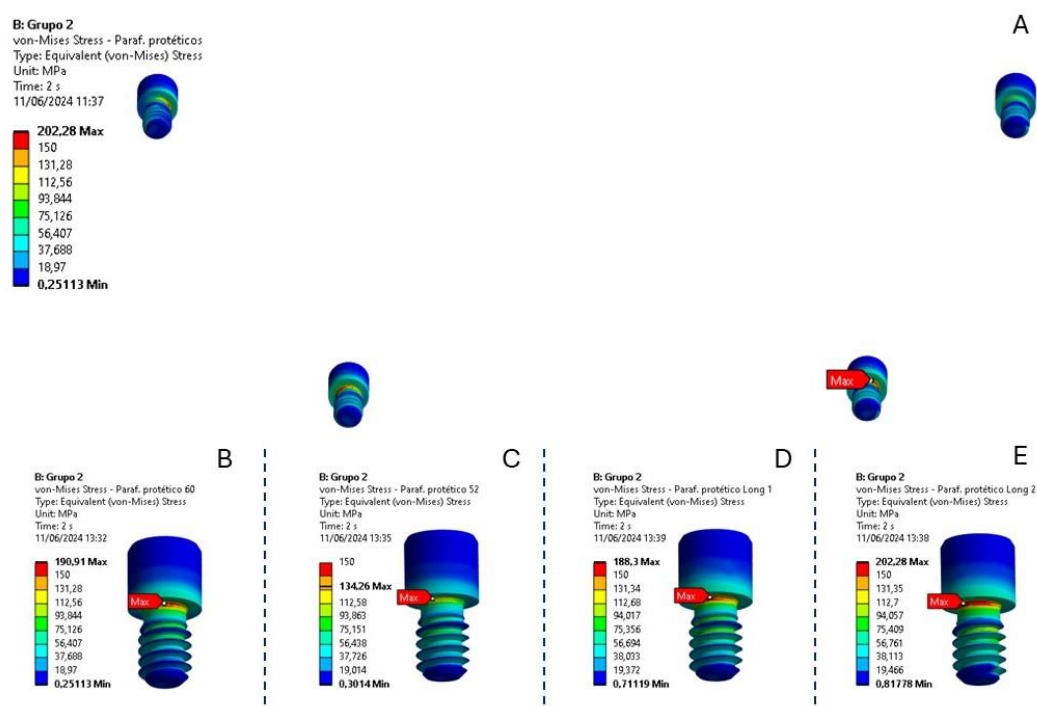
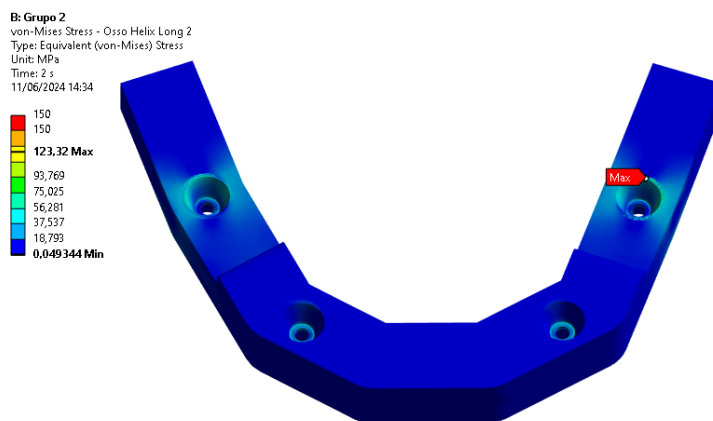


Figure 8 - Stress distribution in prosthetic screws. The red areas mean higher values and the blue ones, smaller. A) Overview with all prosthetic screws in installation position; B) Approximate view of the prosthetic screw associated with the Zygoma-S implant associated with the 60° Mini Conical Abutment in position 16; C) Approximate view of the prosthetic screw associated with the Zygoma-S implant associated with the 52° Mini Conical Abutment in position 26; D) Approximate view of the prosthetic screw associated with the Helix Long implant in position 13; E) Approximate view of the prosthetic screw associated with the Helix Long implant in position 23.



Finally, the greatest stresses generated in the prosthetic bar are located in the region of the zygomatic implants, with a maximum value of 123.32 MPa (Figure 9).

Figure 9 - Stress distribution on the prosthetic bar.



The maximum von Mises values in each element of the model are described in Table 2. Higher values were found in zygomatic implants than in transnasal implants. On the contrary, it is seen in prosthetic components, where the components associated with transnasal implants presented higher stresses than the components associated with zygomatic implants.

Table 2 – Table of maximum von Mises stresses in each element of the model.

Implant [angulation] [position]	Voltages (Mpa)					
	Bone	Implant	Prosthetic component	Parafuse (prosthetic component)	Prosthetic paraphuse	Prosthetic bar
Zygomatic [60th] [16]	31,18	250,53	150,22	129,77	190,91	123,32
Zygomatic [52nd] [26]	20,96	212,48	148,35	119,42	134,26	
Helix Long [0°] [13]	9,11	150,78	237,95	-	188,30	
Helix Long [0°] [23]	6,90	152,47	228,83	-	202,28	

DISCUSSION

In this study, we evaluated the mechanical behavior of the hybrid all-on-4 technique by associating smooth zygomatic implants with extra-long transnasal implants through the distribution of stresses generated by the finite element method. Finite element analysis is a non-invasive method that can be performed whenever necessary at no extra cost and quickly. When coupled with clinical data, it helps confirm the safety and performance of different dental implant installation techniques.

The quad-zygoma technique is an alternative for patients without enough bone in the anterior region to be treated by the hybrid all-on-4 technique with conventional implants. However, this technique is riskier and requires greater operator experience. Thus, as an option, the hybrid all-on-4 technique can be used with extra-long implants with transnasal anchorage(4). In this approach, the first step in performing transnasal osteotomy involves elevating the nasal mucosa of the distal and inferior nasal walls, using specific curettes for paranasal sinuses. Drilling is performed only after accurately identifying the position of the inferior nasal concha and the conchal crest of the maxilla, which define the location of the apex of the transnasal implant. Throughout the process, the nasal mucosa is carefully protected by means of periosteal detachers or sinus curettes, ensuring that the drills do not cause damage to the tissue(3).

To facilitate the planning of atrophic maxillary rehabilitation, studies theoretically divide the maxilla into regions to facilitate the visualization of anatomical structures and one of these regions is known as the "Z-point". This "Z-spot" is the region between the lateral wall of the nasal cavity and the medial wall of the maxillary sinus, at the level of the inferior nasal concha. Extra-long implants can be anchored in this region as long as there is a minimum of 3 mm of bone for anchorage. In addition, a minimum bone height of 4 mm is required between the alveolar ridge of the maxilla and the nasal cavity to ensure sufficient primary stability for immediate loading. This technique should be avoided in patients with a very large nasal cavity in the laterolateral direction (15).

The technique is not yet widely disseminated in the literature, but some clinical cases demonstrating the feasibility and safety of the technique have already been published. Nunes et al. (2024) treated three patients with the hybrid all-on-4 technique using two zygomatic implants and two extra-long implants with transnasal anchorage. Implant survival was 100%. There were no biological complications and only one acrylic crown fractured in a temporary prosthesis. In two other case reports, the same procedure was performed without complications(15,16). A finite element analysis study evaluating this technique can complement the understanding of the mechanics involved. In view of this, Almeida et al. (2021)(16) suggested conducting finite element analysis studies with the purpose of analyzing the stresses generated by extra-long transnasal implants in adjacent bone tissues, prosthetic components, and prosthetic screws.

In the present study, the maximum stresses found in each element of the evaluated model do not exceed the strength limit of the materials, which is 170 MPa for the type of

bone studied, 483 MPa for grade 4 titanium and 795 MPa for titanium alloy, according to table 1 mentioned above. Indicating that the system resists the stresses applied to it.

The higher stresses found in zygomatic implants can be explained by the application of forces on the cantilever. In this study, 100N of force was applied bilaterally to the cantilever. This application generates a lever movement that compresses the posterior implants (zygomatic) and tensions the anterior implants (long implants), in this way, the distribution of tensions in the zygomatic implant is more expressive. In addition, a greater distribution of stresses in the palatal region of zygomatic implants can be observed. In inclined implants, occlusal forces fall in parallel, increasing lateral tensions and momentum(17) leading to a concentration of tension in the palatal region of the implant, whereas in straight implants, such as transnasal implants, the tensions are evenly distributed in the region of the implant cone.

It is possible to observe that the tensions were higher in the prosthetic components associated with the transnasal implants. As the lever arm generated by the cantilever pulls the transnasal implants, the thread region of the prosthetic component undergoes greater effort to maintain the component-implant connection. Thus, the maximum stresses on the prosthetic components of transnasal implants are more expressive than the stresses of the components associated with zygomatic implants. The stress distribution was similar between the 52 and 60° prosthetic components, and the highest stresses were located in the elbow region of the component and in the region where the screw is seated. This higher stress in the region of the bolt settlement is due to the preload that these bolts receive with the application of torque in the installation and in the elbow region is due to the sudden change in geometry.

The limitations of this study are the same as those of any finite element study, not mimicking 100% what happens in clinical practice. The authors recommend that clinical studies be conducted to prove the safety and performance of the hybrid all-on-4 technique using zygomatic implants and extra-long implants with transnasal anchorage. In addition, in this study, oblique forces from lateral movements during chewing were not considered.

CONCLUSION

The present study revealed that the rehabilitation of severely atrophic maxillae by the hybrid all-on-4 technique using two zygomatic implants and two extra-long implants with transnasal anchorage is biomechanically favorable and reliable. Additionally, the

maximum stresses found in each element of the evaluated model do not exceed the resistance limit of the materials, indicating that the system resists the stresses applied to it.

REFERENCES

1. Ali SA, Karthigeyan S, Deivanai M, Kumar A. Implant rehabilitation for atrophic maxilla: a review. *The Journal of Indian Prosthodontic Society*. 2014;14:196–207.
2. Andre A, Dym H. Zygomatic implants: a review of a treatment alternative for the severely atrophic maxilla. *Atlas Oral Maxillofac Surg Clin North Am*. 2021;29(2):163–72.
3. Şahin O. Treatment of severely atrophic maxilla by using zygomatic, pterygoid, and transnasal implants. *Journal of Craniofacial Surgery*. 2024;35(2):e145–6.
4. Nunes M, de Araújo Nobre M, Camargo V. All-on-4 Hybrid with Extra-Long Transnasal Implants: Descriptions of the Technique and Short-Term Outcomes in Three Cases. *J Clin Med*. 2024;13(11):3348.
5. Zupancic Cepic L, Frank M, Reisinger A, Pahr D, Zechner W, Schedle A. Biomechanical finite element analysis of short-implant-supported, 3-unit, fixed CAD/CAM prostheses in the posterior mandible. *Int J Implant Dent*. 2022;8(1):8.
6. Stella JP, Warner MR. Sinus slot technique for simplification and improved orientation of zygomaticus dental implants: a technical note. *International Journal of Oral & Maxillofacial Implants*. 2000;15(6).
7. Tada S, Stegaroiu R, Kitamura E, Miyakawa O, Kusakari H. Influence of implant design and bone quality on stress/strain distribution in bone around implants: a 3-dimensional finite element analysis. *International Journal of Oral & Maxillofacial Implants*. 2003;18(3).
8. De Almeida EO, Rocha EP, Freitas Jr AC, Martin Jr M. Finite element stress analysis of edentulous mandibles with different bone types supporting multiple-implant superstructures. *International Journal of Oral & Maxillofacial Implants*. 2010;25(6).
9. Menacho-Mendoza E, Cedamanos-Cuenca R, Díaz-Suyo A. Stress analysis and factor of safety in three dental implant systems by finite element analysis. *Saudi Dent J*. 2022;34(7):579–84.
10. Zhang C, Wang Y. Biomechanical Analysis of Axial Gradient Porous Dental Implants: A Finite Element Analysis. *J Funct Biomater*. 2023;14(12):557.
11. Wang C, Fu G, Deng F. Difference of natural teeth and implant-supported restoration: A comparison of bone remodeling simulations. *J Dent Sci*. 2015;10(2):190–200.
12. Eskitascioglu G, Usumez A, Sevimay M, Soykan E, Unsal E. The influence of occlusal loading location on stresses transferred to implant-supported prostheses and supporting bone: A three-dimensional finite element study. *J Prosthet Dent*. 2004;91(2):144–50.

13. Haack JE, Sakaguchi RL, Sun T, Coffey JP. Elongation and preload stress in dental implant abutment screws. *Int J Oral Maxillofac Implants*. 1995;10(5):529–36.
14. Lang LA, Kang B, Wang RF, Lang BR. Finite element analysis to determine implant preload. *J Prosthet Dent*. 2003;90(6):539–46.
15. Oh S, Zelig D, Aalam AA, Kurtzman GM. Case report: utilization of Z-Point fixture “Trans-nasal” implants. *Annals of Medicine and Surgery*. 2023;85(5):1959–65.
16. Almeida PHT, Cacciacane SH, Junior AA. Extra-long transnasal implants as alternative for Quad Zygoma: Case report. *Annals of Medicine and Surgery*. 2021;68:102635.
17. Duan Y, Chandran R, Cherry D. Influence of Alveolar Bone Defects on the Stress Distribution in Quad Zygomatic Implant–Supported Maxillary Prosthesis. *International Journal of Oral & Maxillofacial Implants*. 2018;33(3).